0 0 0 0 4 4 0 0 2 0 4

Submitted to Physical Review A

RECEIVED
BERKELEY LABORATORY
DEC 2 1975
LIBRARY AND
DOCUMENTS SECTION

LBL-4307
Preprint c.1

K VACANCY PRODUCTION BY 4.88 GeV PROTONS

R. Anholt and the TOSABE Group

September 1975

Prepared for the U. S. Energy Research and
Development Administration under Contract W-7405-ENG-48

For Reference

Not to be taken from this room

LAWRENCE BERKELEY LABORATORY
UNIVERSITY OF CALIFORNIA
BERKELEY

LBL-4307
c.1

DISCLAIMER

This document was prepared as an account of work sponsored by the United States Government. While this document is believed to contain correct information, neither the United States Government nor any agency thereof, nor the Regents of the University of California, nor any of their employees, makes any warranty, express or implied, or assumes any legal responsibility for the accuracy, completeness, or usefulness of any information, apparatus, product, or process disclosed, or represents that its use would not infringe privately owned rights. Reference herein to any specific commercial product, process, or service by its trade name, trademark, manufacturer, or otherwise, does not necessarily constitute or imply its endorsement, recommendation, or favoring by the United States Government or any agency thereof, or the Regents of the University of California. The views and opinions of authors expressed herein do not necessarily state or reflect those of the United States Government or any agency thereof or the Regents of the University of California.

0 0 0 0 4 4 0 3 2 3 5

LBL-4307

K VACANCY PRODUCTION BY 4.88 GeV PROTONS*

R. Anholt, and the TOSABE† Group

Lawrence Berkeley Laboratory
University of California
Berkeley, California 94720

ABSTRACT

Cross sections for K vacancy production by 4.88 GeV protons on elements between Ni and U have been measured. These cross sections lie a factor of two above the Binary Encounter Approximation predictions and above the Plane Wave Born Approximation predictions also. To explain these deviations, we argue that a distant collision term must be added to the BEA expression. Our experimental results agree well with the augmented theory.

---

*Work done under the auspices of the U. S. Energy Research and Development Administration.

†Members also participating in these experiments were S. Nagamiya, J.O. Rasmussen, H. Bowman, J. Ioannou-Yannou, E. Rauscher. TOSABE stands for Tokyo, Osaka, Berkeley collaboration.

I. INTRODUCTION

In recent years much effort has been devoted to measuring cross sections for K vacancy production by energetic protons and alpha particles in medium heavy and heavy elements.[1] Most of this work has been done at energies between a hundred keV and 30 MeV per nucleon. Three theories exist that predict the cross sections: the Binary Encounter Approximation (BEA),[2,3] the Plane Wave Born Approximation (PWBA),[4] and the Semiclassical Approximation (SCA).[5] To first order, these theories predict that the K vacancy cross sections should fit on a universal curve and should be a function only of the K shell binding energy U_K, the atomic number of the projectile Z_1, and the ratio of the projectile velocity to the velocity of the electron in the K shell v_1/v_K. Nearly all of the data taken fits the universal curve to within approximately a factor of two.

K vacancy production by very relativistic protons has not yet been examined.[1] Non-relativistically, the cross sections depend on just the ratio v_1/v_K and hence one can actually examine the high energy part of the universal curves by measuring K vacancy production cross sections by moderately energetic protons on very light elements. Thus far, though, these non-relativistic measurements have not exceeded $v_1/v_K \approx 2$.[1] With 4.88 GeV protons, it is possible to obtain $v_1/v_K \approx 5$ (on Ni) which is clearly much larger than any previous measurement. In addition to the large v_1/v_K, however, there is the possibility that additional relativistic effects on the cross sections may be investigated. Previously the highest energy work has been done with 160 MeV protons[6] where no dramatic deviation from the non-relativistic PWBA theory was found. The cross sections simply decreased roughly as the inverse square of v_1/v_K as predicted by the PWBA

and BEA theories. The authors of that work compared their results with relativistically calculated cross sections for K vacancy production by incident electrons suggesting that at proton energies slightly higher than 160 MeV, relativistic effects may cause the cross section to rise again.

We originally undertook this work in order to test whether such a rise in the cross section may be observed at 4.88 GeV. In Section II of this paper we present our experimental work and final cross sections which are higher than the BEA and PWBA theory predictions. To explain these deviations we show that a distant collision term must be added to the BEA cross section. In the BEA theory, electrons are ejected from the K shell when they undergo Rutherford scattering by the projectile in collisions where the impact parameter is generally less than the target K-shell radius a_K. However, contributions can come from collisions with impact parameters greater than a_K where energy is transferred from the projectile to the bound electron through the virtual radiation field of the moving projectile. We compare the BEA+ distant collision cross section with our results and others in Section IV.

II. EXPERIMENT

The experimental configuration is schematically illustrated in Fig. 1. Protons of 4.88 GeV from the Lawrence Berkeley Laboratory Bevatron passed through a 0.0254 mm Ag monitor foil, a 0.00608 to 0.0508 mm target foil, a scintillation paddle, ion chamber, and a TV monitor paddle with negligible energy loss. A horizontally placed Si(Li) detector viewed the target at right angles to the beam, and a Ge(Li) planar detector facing upward, likewise viewed the target at right angles to the beam. The target was tilted vertically

by 45° and was rotated by 45° so that its normal was 60° to the beam and its plane face was 45° from both the Si(Li) and Ge(Li) detectors. Both detectors also viewed the Ag monitor foil, which was placed 10 cm upstream from the target. To make deadtime corrections, pulses from each detector fired a fast discriminator which supplied one pulse every hundred pulses to trigger a pulser on the opposite detector. The number of pulses triggered (p_{in}) was recorded and later the number of pulses counted (p_c) was found. The deadtime correction (p_{in}/p_c-1) varied between 0.4% and 50%.

To monitor the beam intensity, we relied on an ion chamber coupled to an electrometer and integrator to integrate the relative intensity of the beam from run to run. The absolute intensity of the beam was found by irradiating a 0.95 cm thick graphite target and then we off-line counted the annihilation radiation from the β^+decay of ^{11}C formed in the $^{12}C(p,pn)\,^{11}C$ reaction. Since the ^{11}C reaction has a known (interpolated) cross section for 4.88 GeV protons, 28 ± 0.6mb[7,8] the absolute number of protons passing through the carbon target and ion chamber could be found. Seven calibration runs were taken. The measured number of particles per ion chamber reading varied by less than 2%.

To obtain cross sections insensitive to the uncertainty in the detector deadtime, we measured all of the x-ray yields relative to the yield of Ag Kα x-rays observed in the monitor foil which, together with the detectors, remained in a fixed position throughout the entire experiment. For some 40 runs we averaged the quantity:

$$x = \frac{C(AgK\alpha)}{I.C.} \; \frac{p_{in}}{p_c} \qquad (1)$$

where C(AgKα) is the counts observed in the monitor foil, I.C. is the ion chamber reading, and p_{in}/p_c is the pulser measured deadtime correction.

The yield for an x-ray of energy E_x was found by:

$$Y = \frac{C(E_x)}{C(AgK\alpha)} \frac{\langle x \rangle A}{F(E_x)P} \quad \text{photons/proton} \qquad (2)$$

where P is the number of protons per ion chamber reading, $F(E_x)$ is the detector efficiency, $C(E_x)$ is the counts observed in the x-ray peak of energy E_x, and A is the correction for air and Be attenuator absorption.

To obtain cross sections, this yield was divided by the target atom density and effective thickness $[1 - \exp(-\mu t)]/\mu$ where t is the thickness of the tilted target and $\mu(E_x)$ is the attenuation coefficient of the target fluorescent x-rays in the target material.[9] The cross sections for the Kα and Kβ peaks (where separable) were then added, and the neutral atom fluorescent yield[10] was used to convert the x-ray cross sections to vacancy cross sections.

The uncertainties in these procedures were as follows:

(1) Protons per ion chamber reading (counting statistics, ^{11}C cross section, β^+ counter efficiency, graphite target thickness): ± 4%

(2) Detector efficiency: ± 8% Si(Li), ± 14% Ge(Li)

(3) Average number of deadtime corrected Ag Kα counts per ion chamber reading ($\langle x \rangle$): ± 13% Ge(Li), ± 7% Si(Li)

(4) Target angle, thickness, absorption coefficient: ± 2%

(5) Counting statistics including variation from run to run: ± 2 - 10%

In addition, one other correction for target thickness needs to be made. Plots of the cross sections as a function of target thickness

(fig. 2) show that there is a definite trend for the observed cross sections to increase with target thickness. This is due mainly to two secondary processes:[6] (1) protons making energetic secondary electrons in the target which excite K vacancies, and (2) protons making secondary electrons which emit bremsstrahlung radiation in collisions with other target nuclei which photoelectrically excites K vacancies.
For thin targets the former process increases the cross section linearly with target thickness, the later process increases it quadratically.

To adjust our measured cross sections to zero target thickness we have used theoretical, though approximate, expressions for processes (1) and (2) and have semi-empirically fit these expressions to the data obtained when many different target thicknesses were used. The uncertainty in this correction is at least as large as the correction itself which in no case was more than 12%. The final cross sections are listed in Table I together with the correction for finite target thickness and the total uncertainty.

III. THEORY

Relativistic Stationary Electron Approximation (RSEA)

For the extremely high energies used in our experiment, the existing Binary Encounter Approximation (BEA),[2,3] Plane Wave Born Approximation (PWBA),[4] and Semi-Classical Approximation (SCA)[5] theories do not handle relativistic effects correctly, though they generally do take proper account of the initial motion of the struck electron, Coulomb deflection of the projectile, and other non-relativistic effects. We shall introduce the RSEA theory which will handle the relativistic terms correctly, but not the initial motion of the K electron.

We consider the K electron to be stationary with respect to the moving projectile, which is equivalent to considering $v_1 \gg v_K$ where v_1 is the projectile velocity and v_K is the K electron velocity. Vacancies can be created if the projectile scatters the K electron transferring energy in excess of the K binding energy. At relativistic energies the usual Rutherford scattering formula should be replaced by the McKinley-Feshbach formula[11] which, written differential in the energy transfer ε, is:

$$\frac{d\sigma}{d\varepsilon} = \frac{2\pi e^4}{mc^2\beta^2}\,\frac{Z_1^2}{\varepsilon^2}\left\{1 - \beta^2\frac{\varepsilon}{\varepsilon_m} + \alpha Z_1\pi\beta\left[\left(\frac{\varepsilon}{\varepsilon_m}\right)^{\frac{1}{2}} - \frac{\varepsilon}{\varepsilon_m}\right]\right\} \qquad (3)$$

where $\alpha = 1/137$, $\beta = v/c$, ε_m is the maximum energy transfer $2mc^2\beta^2\gamma^2$ to order $\frac{m_e}{M}\gamma\beta$, and M is the projectile mass. The first term in this expression is the familiar Rutherford scattering cross section while the first and second terms make up the well known Mott result.[12] Mott's formula has been expanded in powers of $Z_1\alpha$ by McKinley and Feshbach[13] and the third term in this expression is correct to third order in $Z_1\alpha$. The vacancy production cross section per atom is:

$$\sigma_K = 2\int_{U_K}^{\varepsilon_m}\frac{d\sigma}{d\varepsilon}\,d\varepsilon \qquad (4)$$

where U_K is the K binding energy and the factor of 2 is included because there are two K electrons per atom. The resulting cross section is

$$\sigma_K = \frac{4\pi Z_1^2 e^4}{mc^2\beta^2 U_K}\left[1 - \frac{U_K}{\varepsilon_m} - \frac{U_K\beta^2}{\varepsilon_m}\,\ln\left(\frac{\varepsilon_m}{U_K}\right) + \frac{\pi\alpha Z_1\beta U_K}{\varepsilon_m}\left(2\left(\frac{\varepsilon_m}{U_K}\right)^{\frac{1}{2}} - 2 - \ln\left(\frac{\varepsilon_m}{U_K}\right)\right)\right] \qquad (5)$$

Figure 3 plots the second and third terms in this expression in units of the leading term $4\pi Z_1^2 e^4/mc^2\beta^2 U_K$ for various proton energies. The $Z_1\alpha$ term increases in importance with larger values of U_K and Table II gives the contribution for nearly the largest value of U_K considered in this work. The corrections to the leading term, which is essentially the Rutherford term, are very small for protons. The reason for this may be seen by examining Eq. (3). The cross section falls off as ε^{-2}; therefore, the important part of the cross section is for the smallest energy transfer U_K. The relativistic terms enter as the ratio $\varepsilon/\varepsilon_m$ or U_K/ε_m which is small compared to unity, e.g., 0.05, 0.0055, 0.0091 for U_K = 50 keV and E_1 = 0.4, 2 and 6 GeV/amu respectively. Hence, the relativistic terms clearly give insignificant contributions to the non-relativistic Rutherford cross section. This leads us to believe that we can, to good approximation, estimate K vacancy production in collisions involving relativistic protons by the non-relativistic expression, where the projectile energy is replaced by $E_1 = \frac{1}{2}mc^2\beta^2$.

Let us use this prescription to modify the BEA theory[2]. The BEA theory accounts for the Rutherford scattering of an electron of velocity $\vec{v}_2$ by a projectile with velocity $\vec{v}_1$ giving an energy transfer ε. A formula like (2) is used except that an additional average over the direction of $\vec{v}_1$ and $\vec{v}_2$ and the initial electron speed v_2 is done. The probability for an electron traveling with velocity v_2 is $|\psi(v_2)|^2$, where $\psi(v_2)$ is the Fourier transform of the K shell configuration wave function. We can compare the RSEA theory. The BEA cross section can be written as:[3]

$$\sigma_K = \frac{2\pi Z_1^2 e^4}{U_K^2} G(v_1/v_K) \qquad (6)$$

where v_1/v_K will be replaced by $[\frac{1}{2} mc^2\beta^2/U_K]^{\frac{1}{2}}$. Analytical expressions for G are available, and since $v_1/v_K > 1$, we may approximate G by neglecting terms of order v_K/v_1 obtaining

$$\sigma_K = \frac{4\pi Z_1^2 e^4}{mc^2\beta^2 U_K} (1 + 0.67 \ln(2.7 + v_1/v_K)) \qquad (7)$$

Except for the logarithmic term this is the same as was obtained in the RSEA theory when terms of order U_K/ε_m are neglected. The logarithmic term in the BEA theory comes from including the initial motion of the struck electron.

The above arguments are meant to show that Rutherford scattering adequately describes the K electron-projectile interaction and thus the BEA theory should work if we use the prescription of replacing E_1 by $\frac{1}{2}mc^2\beta^2$. We have examined Gerjuoy's original formulation[14] of the BEA formulas to see if replacing E_1 by $\frac{1}{2}mc^2\beta^2$ and continuing to treat the initial electron motion non-relativistically is incorrect. In his work momenta and velocities were used and E_1 appears in the final results by putting $E_1 = \frac{1}{2}M v_1^2$ This energy was multiplied by the reduced mass divided by M which, both relativistically and non-relativistically, is approximately the rest electron mass when the electron velocity is small. It seems to us to be correct to replace E_1 by $\frac{1}{2}mc^2\beta^2$ in Gerjuoy's BEA expression.

K Vacancy Production in Distant Collisions

In the theory of stopping powers[11,15] and K vacancy production by incident electrons,[16] the cross sections are often divided into a close collision part and a distant collision part. The dividing line between the two is often at an impact parameter b around the electron shell radius, in

our case a_K. For collisions with $b < a_K$, energy is transferred from the projectile to the K electron by Rutherford[11] (heavy particle + electron) or Möller[16] (electron-electron) scattering as described above. In the distant collisions, energy is transferred via the radiation field of the moving projectile.

We calculate the part due to distant collisions by using the method suggested by Williams.[17] There are, of course, other methods which are essentially equivalent and have been used in the stopping power formulas, but Williams' method is most simple and has already enjoyed considerable success predicting K vacancy cross sections with relativistic electrons.[16]

The field of a projectile passing by an electron with an impact parameter b has a spectrum of virtual quanta given by the square of the Fourier transform of the time dependent electric field:

$$\frac{dN}{d(\hbar\omega)}(\omega,b) = \frac{c}{2\pi(\hbar\omega)} \; |\vec{E}(\omega,b)|^2 \tag{8}$$

where

$$\vec{E}(\omega,b) = \int_{-\infty}^{\infty} dt \; \vec{E}\,(t)\; e^{i\omega t}$$

and the time integral is over a trajectory with a given projectile velocity and electron-projectile impact parameter. To obtain the total spectrum, we integrate over impact parameter:

$$\begin{aligned} \frac{dN(\omega)}{d(\hbar\omega)} &= \int_{b_{min}} 2\pi b db \; \frac{dN(\omega,b)}{d(\hbar\omega)} \\ &= \frac{2}{\pi} \frac{Z_1^2 e^2}{c\hbar\omega\beta^2} \left[x\, K_0(x) K_1\,(x) - \tfrac{1}{2}\beta^2 x^2 (K_1^2(x) - K_0^2(x)) \right] \end{aligned} \tag{9}$$

where $x = \frac{\omega b_{min}}{\gamma v}$, $\gamma = (1-\beta^2)^{-\frac{1}{2}}$, and $K_n(x)$ are the usual modified Bessel functions. For $x \ll 1$, the spectrum can be approximated by:

$$\frac{dN}{d(\hbar\omega)} = \frac{2}{\pi} \frac{Z_1^2 e^2}{c\hbar\omega\beta^2} \left[\ln \left(\frac{1.123\gamma}{\omega_x b_{min}} v \right) - \beta^2/2 \right] \tag{10}$$

So far we have not specified b_{min}. A non-zero choice of b_{min} must be made in order to obtain a non-divergent spectrum. The choice usually made in these problems is to use the radius of electron shell from which excitation occurs which in this case is the K shell radius a_K. The argument for this choice is that for impact parameters less than a_K the expansion of the interaction into multipoles fails and the dipole approximation can no longer be trusted. Other arguments have been given.[11] Unfortunately, the final results will not be insensitive to the choice of b_{min}.

Photons of energy $\hbar\omega_x > U_K$ can photoelectrically excite K electrons giving a net cross section

$$\sigma(b > a) = \int_{U_K}^{\omega_0} \sigma_{PE}(\omega_x) \frac{dN}{d\omega_x} d\omega_x \tag{11}$$

where ω_0 is the cutoff frequency, $1.123\ \gamma\beta c/a_K$, and σ_{PE} is the photoelectric cross section per atom approximated by

$$\sigma_{PE} = \frac{84}{(\alpha^3 Z^2)} \left(\frac{U_K}{\hbar\omega_x} \right)^4 \frac{\exp(-4n \cot^{-1} n)}{(1 - e^{-2\pi n})} \text{ barns} \tag{12}$$

with $n = \left[\hbar\omega_x/U_K - 1 \right]^{-\frac{1}{2}}$. Following Kolbensvedt,[16] (11) is integrated (with approximations) and we find

$$\sigma(b > a) = \frac{141 Z_1^2}{U_K \beta^2} \left\{ \ln\left(\frac{(\beta\gamma)^2 608}{U_K}\right) - \beta^2 \right\} \text{ barns} \tag{13}$$

where U_K is in keV.

As long as we are careful about not double counting, the total K vacancy cross section can be written as

$$\sigma = \sigma(b < a) + \sigma(b > a) \tag{14}$$

where $\sigma(b < a)$ can be either the BEA, RSEA, or PWBA cross section. In deriving $\sigma(b > a)$ we do not count impact parameters less than a_K. In the RSEA theory, the largest impact parameter is when $\varepsilon(b) = U_K$ or

$$b_{max} = \left(\frac{Z_1 e^2}{mc^2 \beta^2}\right) \left(\frac{\varepsilon_m}{U_K} - 1\right)^{\frac{1}{2}} \tag{15}$$

Neglecting unity with respect to ε_m/U_K we obtain the maximum impact parameter in the RSEA (and also BEA) theory:

$$b_{max} \cong \frac{2\alpha Z_1 \gamma}{\beta} a_K \tag{16}$$

Equation (14) is thus invalid for protons if $\beta \lesssim 0.01$ or $\gamma > 68$. Neither of these cases are of serious interest in the work.

IV. DISCUSSION

Figure 3 shows the ratio of our cross sections to (a) the RSEA results, (b) the BEA theory results,[1] (c) the BEA + distant collision results, and

(d) the PWBA results.[18] The RSEA ratio (a) is higher than the BEA ratio (b) and this is because the BEA cross sections are larger than the RSEA cross sections by the contribution from the logarithmic term in eq. (5) which comes from including the initial motion of the struck electron. The RSEA, BEA, and PWBA cross sections all lie a factor of 1.4 to 3. times lower than our experimental results, and we would be hard pressed to explain these large factors without adding the additional distant collision term. Adding this term clearly brings the theory in line with our experimental results.

The distant collision term is not a purely relativistic phenomenon, but should contribute whenever the velocity is large. When $\beta^2 << 1$ $\sigma(b > a)$ can be written in such a way as to display the universal scaling dependence that is familiar in the BEA theory.

$$\sigma(b > a) \frac{U_K^2}{Z_1^2} = 3.6 \times 10^{-20} \frac{U_K \lambda}{E_1} \ln\left(\frac{2.38 E_1}{\lambda U_K}\right) \text{cm}^2 \text{ keV}^2 \qquad (17)$$

where λ is the ratio of the projectile mass to the electron mass and E_1 is the projectile kinetic energy. This curve is shown in Fig. 5 together with the BEA curve[1] and the sum of the BEA + distant collision cross sections. In this figure we also show some 2-30 MeV p + Ca, Ti and Ni[19] and some 3-80 MeV α + Fe[20] data. For reduced velocities around unity, the distant collision term increases the cross section by about 30% and it is debatable whether it improves agreement between theory and experiment. For $E_1/\lambda U_K < 0.4$ eq. (17) implies that the distant collision cross section is zero since the argument of the logarithm is less than unity. This is an artifact of the small argument approximations to the Bessel functions in eq. (9) and the cross section is expected to be non-zero for small velocities when more accurate calculations are done.

At near relativistic energies, it is not possible to plot data on a single-parameter, universal curve like that shown in fig. 5. At extreme relativistic energies however, it is possible using the RSEA expression (5) for the close collision cross section and (13) for the distant collision cross section to obtain an approximate single parameter expression. The total cross section is:

$$\sigma = \frac{510 Z_1^2}{\beta^2 U_K} + \frac{141 Z_1^2}{\beta^2 U_K}\left[\ln\left(\frac{(\beta\gamma)^2\ 608}{U_K}\right) - \beta^2\right] \text{ barns} \tag{18}$$

where the higher order, relativistic terms in the RSEA expression have been neglected. Replacing the last factor of β^2 in this expression with unity, we can obtain:

$$\frac{\sigma U_K^2}{Z_1^2\gamma^2} = \frac{1.302 \times 10^{-19}}{\gamma^2 V^2}\left[1 + 0.2761(\ln(2.38\gamma^2V^2)-1)\right] \text{ cm}^2\text{-keV}^2 \tag{19}$$

In other words, $\sigma U_K^2/Z_1^2\gamma^2$ is a function of only the variable γ^2V^2 where $V = v_1/v_K$ and v_1/v_K is defined following eq. (6). Fig. 6 shows this curve and compares with our 4.88 GeV proton data which is the only data thus far available for which the approximation $\beta^2 \approx 1$ is justified. The fit is not very good, and this is mostly because of the failure of the RSEA approximation to give a good K vacancy cross section. At higher energies, the initial electron motion terms that are neglected in making the RSEA should be less important compared to the total cross section which continues to increase as the $\ln\gamma^2$. The fit at even higher energies is therefore expected to be slightly better.

Finally we compare with the 160 MeV proton data of Jarvis et al.[6] in Fig. 7. That system is neither extreme relativistic, nor non-relativistic

hence cannot be plotted on either of our universal curves. Including the distant collision cross section improves the agreement between experiment and theory, for the 160 MeV case, but is not quite so impressive as the considerable improvement in the 4.88 GeV data.

In this work we have used very simple formulas for the distant collision term and we have admittedly not used a proper relativistic version of the BEA cross section so the excellent agreement between theory and experiment displayed in figs. 4,5, and 7 may be somewhat fortuitous. Our purpose, however, has not just been to improve agreement with experiment but to show why these distant collision terms should be included in K vacancy production cross sections by incident protons. Even with 4.88 GeV protons we have not reached the point where this distant collision term makes a large, dramatic difference in the observed cross section. The factor of two deviation is not really that significant considering the average performance of the BEA, PWBA, and SCA theories; such a deviation may possibly be explained by other effects that have previously been examined by others. The ultimate test of whether this term should be included in K vacancy cross section calculations lies either in doing experiments at higher energies or in much more sophisticated, theoretical, relativistic PWBA or BEA calculations. We hope the present work sparks further investigations into these directions.

Finally we show how the BEA + distant collision cross section behaves at even higher energies. Since in the BEA theory, the cross sections depend only on the ratio of the projectile velocity to the K electron velocity, the higher energy behavior of this cross section is expected to be constant for $T \gtrsim 5$ GeV. However, the distant collision term rises like the log γ, hence the total cross section also rises. Figure 8 shows the K cross sections for protons on Sn as a function of kinetic energy up to 10,000 GeV.

It is interesting now to return to the point made by Jarvis et al.[6]. By comparing proton induced K excitation cross section with relativistically calculated electron induced K excitation cross sections they had previously suggested the kind of rise that is shown in this curve. However, the reason why the electron K excitation curve rises is because of the distant collision term. In fact, the behavior of the close collision and distant collision contributions in the electron theory[16] is qualitatively similar to that displayed in fig. 8. The close collision part approaches a constant at high incident electron energies while it is the distant collision contribution that causes the cross section to rise.

Conclusions

Cross sections for K vacancy production by 4.88 GeV protons were measured, and they disagreed significantly with the BEA and PWBA predictions. We argue that the classical BEA theory of K vacancy production is correctly extended to relativistic energies when the correct velocity $v_1 = \beta c$ is used in the scaling parameter $(v_1/v_K)^2$, but the BEA expression only accounts for the cross section from encounters with impact parameter less than the K radius. Besides this a distant collision contribution must be added to the classical BEA cross section. The BEA theory only allows K vacancies to be created by direct close collisions; the projectile Rutherford scatters the K electron, ejecting it into the continuum. In distant collisions, K vacancies may also be made if the electron photoelectrically absorbs radiation from the virtual field of the moving projectile.

While little emphasis has been placed on distant collision contributions to the K vacancy cross sections, the idea of applying this correction

is not new and has been previously considered in calculating stopping powers, K vacancy production cross sections by incident electrons, and even vacancy production by incident heavy ions. In their theory of Z_1^3 polarization effects, Basbas et al.[21] calculated the distant collision term of order Z_1^3, but since they were only interested in deviations from Z_1^2 scaling, they did not consider the Z_1^2 term. The distant collision term adds very little to the total cross section at non-relativistic energies and hence its past neglect is not surprising. As K vacancy cross sections are measured at even higher energies, however, the distant collision contribution will be even more important, and at an energy not too much higher than 4.88 GeV, it will be the close collision contribution that will be negligible.

APPENDIX I: TARGET THICKNESS CORRECTION

Two processes are important: (1) protons make secondary electrons which excite K vacancies in electron-electron collisions, and (2) protons make secondary electrons which emit bremsstrahlung ratiation which photoelectrically excites K vacancies. Other more exotic processes such as proton-target nucleus bremsstrahlung radiation photoelectrically exciting K vacancies and processes involving muons, pions, and Kaons in processes (1) and (2) instead of electrons, play an insignificant role. To obtain theoretical expressions, we make a thin target approximation: whichever direction the secondary electron or bremsstrahlung photon is emitted, it travels through a thickness t/2 without energy loss, where t is the thickness of the target. We have followed the work of Jarvis et al.[6] in deriving these expression. The cross section for process (1) is

$$\sigma_{K(1)} = \frac{n_2 t}{2} \quad \frac{d\sigma}{d\varepsilon} \, d\varepsilon \quad \sigma_{K\varepsilon}(\varepsilon) \tag{A1}$$

where n_2 is the target atom density, $d\sigma/d\varepsilon$ is the secondary electron cross section and $\sigma_{K\varepsilon}$ is the cross section for an electron of energy ε exciting a K vacancy. We use a formula similar to (3) for $d\sigma/d\varepsilon$, but exclude the $Z\alpha$ term. The formula of Green and Cosslett[22] is used to calculate the K vacancy cross section by incident electrons of energy ε:

$$\frac{d\sigma}{d\varepsilon} \cong \frac{2\pi e^4 Z_1^2 Z_2}{mc^2\beta^2\varepsilon^2} \left(1 - \beta^2 \frac{\varepsilon}{\varepsilon_m}\right) \tag{A2}$$

$$\sigma_{K\varepsilon}(\varepsilon) \approx \frac{79{,}200}{\varepsilon U_K} \ln \frac{\varepsilon}{U_K} \text{ barns} \tag{A3}$$

where these terms are described following (3) in the text. The integral in (A1) gives approximately

$$\sigma_{K\,1} = 1.5 \times 10^6 \frac{Z_2}{A} \frac{Z_1^2 t}{\beta^2 U_K^3} \text{ barns} \tag{A4}$$

where t is in gm/cm^2 and U_K is the binding energy in keV. The cross section for process (2) is

$$\sigma_{K2} = \int_{u_K}^{\varepsilon_m} d\varepsilon \frac{d\sigma}{d\varepsilon} \int_{u_K}^{\varepsilon} n_2 \frac{d\sigma(\varepsilon)}{dE_x} \frac{t}{2} dE_x P_{PE}(E_x) \tag{A5}$$

where the bremsstrahlung[6,23] cross section is approximately given by

$$\frac{d\sigma}{dE_x}(\varepsilon, E_x) = \frac{1.38 Z_2^2}{\varepsilon E_x} \text{ barns keV}^{-1} \tag{A6}$$

and the photoelectric excitation probability is given by

$$1 - \frac{1 - e^{-\mu t/2}}{\mu t/2} \tag{A7}$$

where $\mu(E_x)$ is parameterized as $j\mu(U_K) \frac{U_K}{E_x}^n$; where j is the jump ratio at the K edge, $\mu(U_K)$ is the absorption coefficient on the high side of the edge,[9] and the fall off of the absorption coefficient for $E_x > U_K$ is parametrized as $(U_K/E_x)^n$ where n is some coefficient. The results are relatively insensitive to n and we take it to be e. The resulting cross section is then

$$\sigma_{K2} \approx 5.3 \frac{Z_1^2 Z_2^3 j\mu(\varepsilon_K) t^2}{A_2 \beta^2 U_K^2} \text{ barns} \tag{A8}$$

To account for the factors neglected in deriving these expressions we use experimental data to fit the observed thickness dependence of several cross sections to

$$\sigma_K = \sigma_{K0} + x\sigma_{K1} + y\sigma_{K2}$$

and values of x and y are found which are smoothly interpolated with Z_2. The resulting dependence for Ni and Au is shown in Fig. 2. Given the uncertainty in the data, and in the approximations made to obtain these theoretical expressions, we concede considerable uncertainty in this procedure, but make the corrections as best that can be done with our data. In no case is the correction greater than 12% of the total cross section which is within the error bars already set.

TABLE I. K vacancy cross sections from 4.88 GeV protons

Z_2	σ (barns)	Finite Target thickness correction
Ni	210 ± 25	2.2%
Zr	102 ± 12	4
Mo	94 ± 12	5.6
Ag	58 ± 10	11.8
Tb	31 ± 7	10.7
Ta	22 ± 4	6.7
Pt	18 ± 4	0.7
Au	17 ± 3	2.8
Pb	15 ± 3	2.7
U	11 ± 3	1.9

TABLE II. Maximum contribution of $Z_1\alpha$ term in eq. (5).
U_K = 100 keV

E_1 GeV/a.m.u.	projectile H	He	Ne	Ar
0.4	0.4%	0.8%	4.2%	7.5%
2.	0.3	0.6	3.1	5.7
6.	0.16	0.32	1.6	2.9

REFERENCES

1. J. D. Garcia, R. J. Fortner, and T. M. Kavanagh, Rev. Mod. Phys. 45, 111 (1973).
2. J. D. Garcia, Phys. Rev. A1, 280 (1970).
3. J. H. McGuire and P. Richard, Phys. Rev. A8, 1374 (1973).
4. E. Merzbacher and H. Lewis, "Encyclopedia of Physics" 34, 166 (Springer-Verlag, Berlin, 1958).
5. J. Bang and J. M. Hansteen, Kgl. Danske Videnskab Selskab, Mat.-Fys. Medd. 31, #13 (1959).
6. O. N. Jarvis, C. Whitehead and M. Shah, Phys. Rev. A5, 1198 (1972), and unpublished Harwell report AERE-R-6612 (1970).
7. J. B. Cummings, Ann. Rev. Nucl. Sci., 13, 260 (1963).
8. For more modern values of the ^{11}C cross section we refer to A. Smith, LBL, private communication (1975).
9. W. H. McMaster, N. Kerr Del Grande and J. H. Mallett, unpublished report UCRL-50174, Section II (1969).
10. W. Bambynek, B. Craseman, R. W. Fink, H.- U. Freund, H. Mark, C. D. Swift, R. E. Price, and P. Venugopula Rao, Rev. Mod. Phys. 44, 716 (1972).
11. J. D. Jackson and R. L. McCarthy, Phys. Rev. B6, 4131 (1972).
12. N. F. Mott, Proc. Roy. Soc. (London) A124, 425 (1929).
13. W. A. McKinley and H. Feshbach, Phys. Rev. 74, 1759 (1948).
14. E. Gerjuoy, Phys. Rev. 148, 54 (1966).
15. J. C. Ashley, R. H. Ritchie and W. Brandt, Phys. Rev. B5, 2393 (1972).
16. H. Kolbenstvedt, J. App. Phys. 38, 4785 (1967).

17. E. J. Williams, Kgl. Danske Videnskab Selskab, Mat.-Fys. Medd. 13, #4 (1935).

18. G. S. Khandewal, B. H. Choi and E. Merzbacher, Atomic Data 1, 103 (1969). The Ni point in fig. 4 involves a 250% extrapolation beyond the end of this table and is consequently uncertain.

19. G. A. Bissinger, J. M. Joyce, E. J. Ludwig, W. S. Moever and S. M. Shafroth, Phys. Rev. A1, 841 (1970).

20. R. L. Watson, C. W. Lewis and J. B. Natowitz, Nucl. Phys. A154, 561 (1970).

21. G. Basbas, W. Brandt, and R. Laubert, Physics Letters 34A, 277 (1971). Also see ref. 15.

22. M. Green and V. E. Cosslett, Proc. Phys. Soc. (London) 78, 1206 (1961).

23. F. Folkmann, C. Gaarde, T. Huus and K. Kemp, Nucl. Inst. Meth. 116, 487 (1974).

FIGURE CAPTIONS

Fig. 1. Schematic diagram showing experimental apparatus layout. FD: fast discriminator, Amp: amplifier, pileup rejector.

Fig. 2. Experimental cross section versus target thickness. Error bars are relative error only. Curve gives approximate to quadratic thickness dependence.

Fig. 3. Cross section calculated using RSEA theory plotted in units of the pure Rutherford contribution: $\frac{4\pi Z_1^2 e^2}{mc^2\beta^2 U_K}$. Includes only the first, second, and third terms of eq. (5).

Fig. 4. Ratios of experimental cross sections for 4.88 GeV protons to theory. Lines are drawn to guide the eye only. Error bars are included for $\sigma_{exp}/(\sigma_{BEA} + \sigma(b > a))$ only.

Fig. 5. Universal curve displaying non-relativistically calculated BEA, $\sigma(b > a)$ and BEA + $\sigma(b > a)$ cross sections. Proton data are from Bissinger et al.[19] and alpha data are from Watson et al.[20]

Fig. 6. Universal curve displaying extreme relativistic cross sections based on the RSEA theory + distant collision terms. Points are from our 4.88 GeV proton measurements. Inclusion of BEA effects of initial K electron motion would bring better agreement between theory and experiment, but they are not convenient to represent in such a scaling law plot. Note in eq. (7) that effects of initial electron motion do not vanish at relativistic projectile velocities, but give a factor that approaches a constant $V = c/v_K$.

Fig. 7. Ratio of experimental cross section to theoretical BEA and BEA + $\sigma(b > a)$ cross section for 160 MeV protons.

Fig. 8. Very high energy behavior of p + Sn cross section calculated using BEA plus distant collision terms.

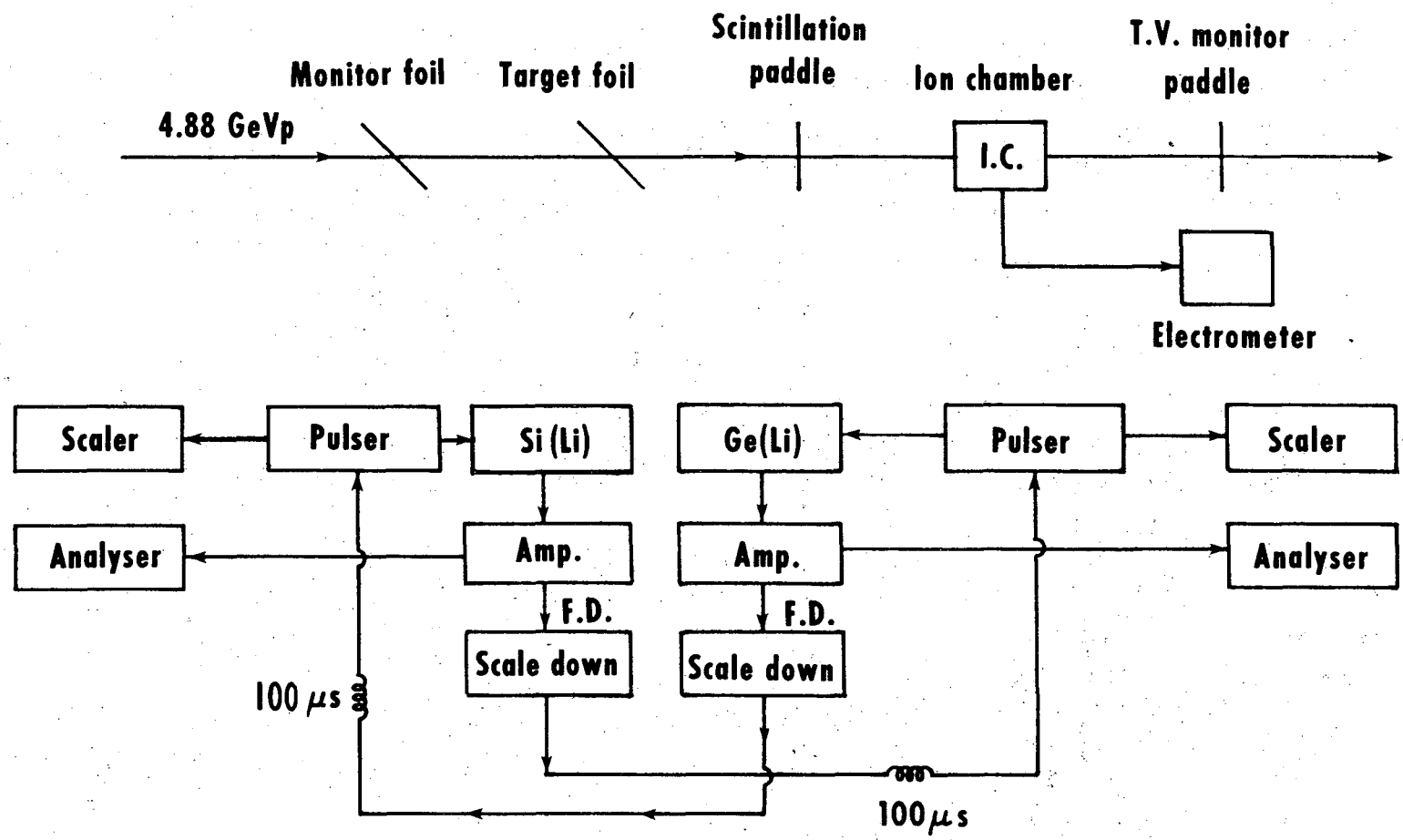

XBL759-3992

Fig. 1

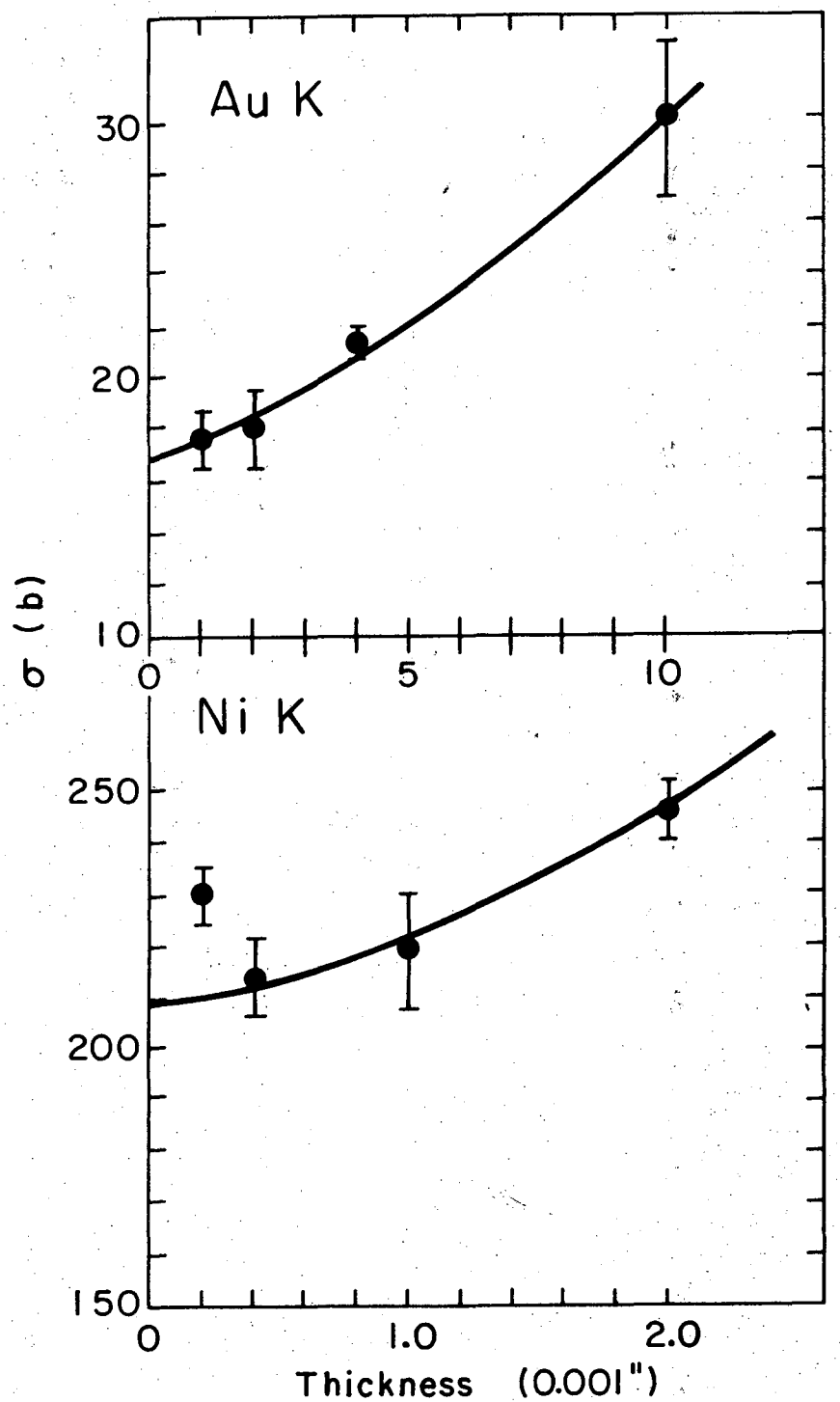

XBL759-3990

Fig. 2

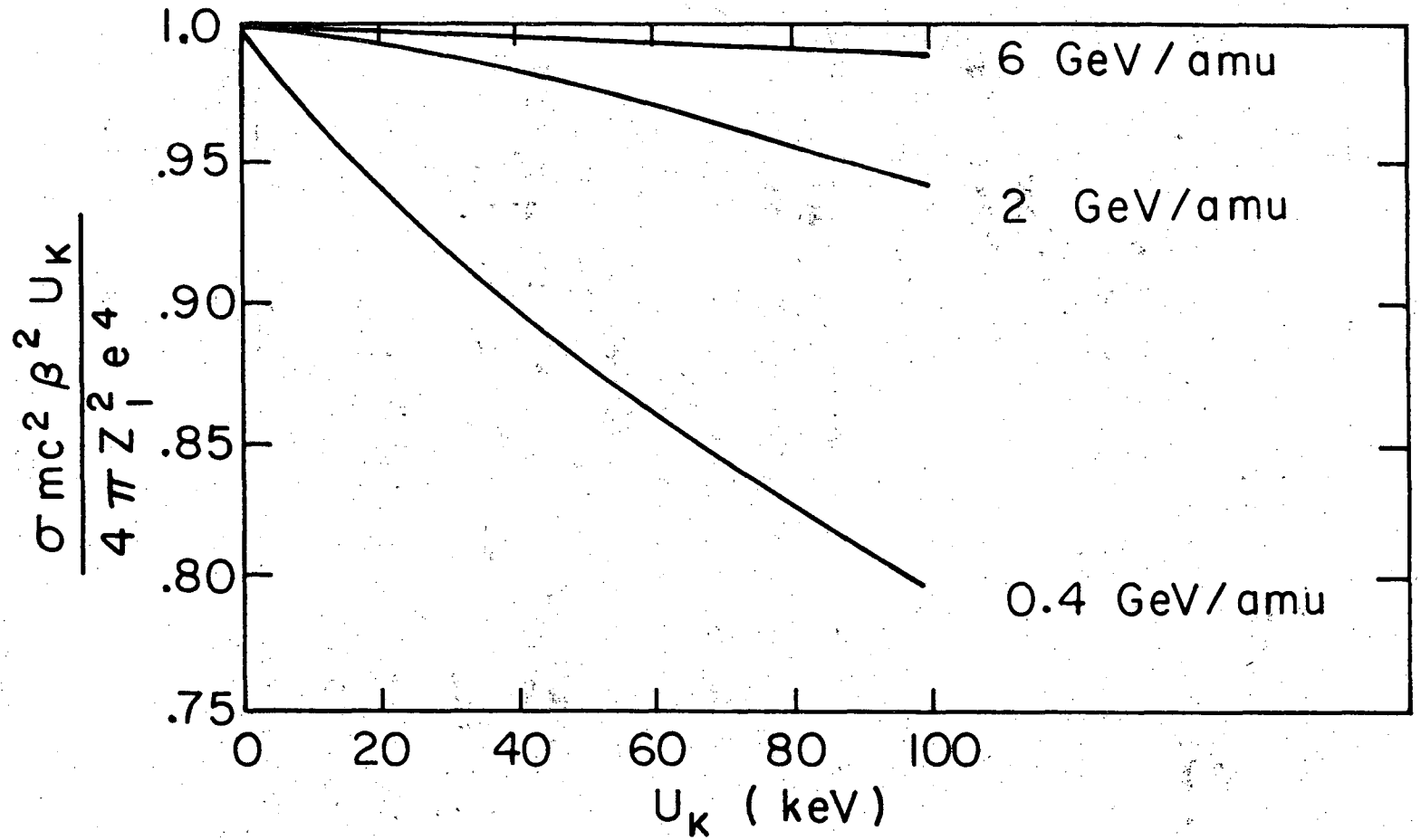

XBL759-3987

Fig. 3

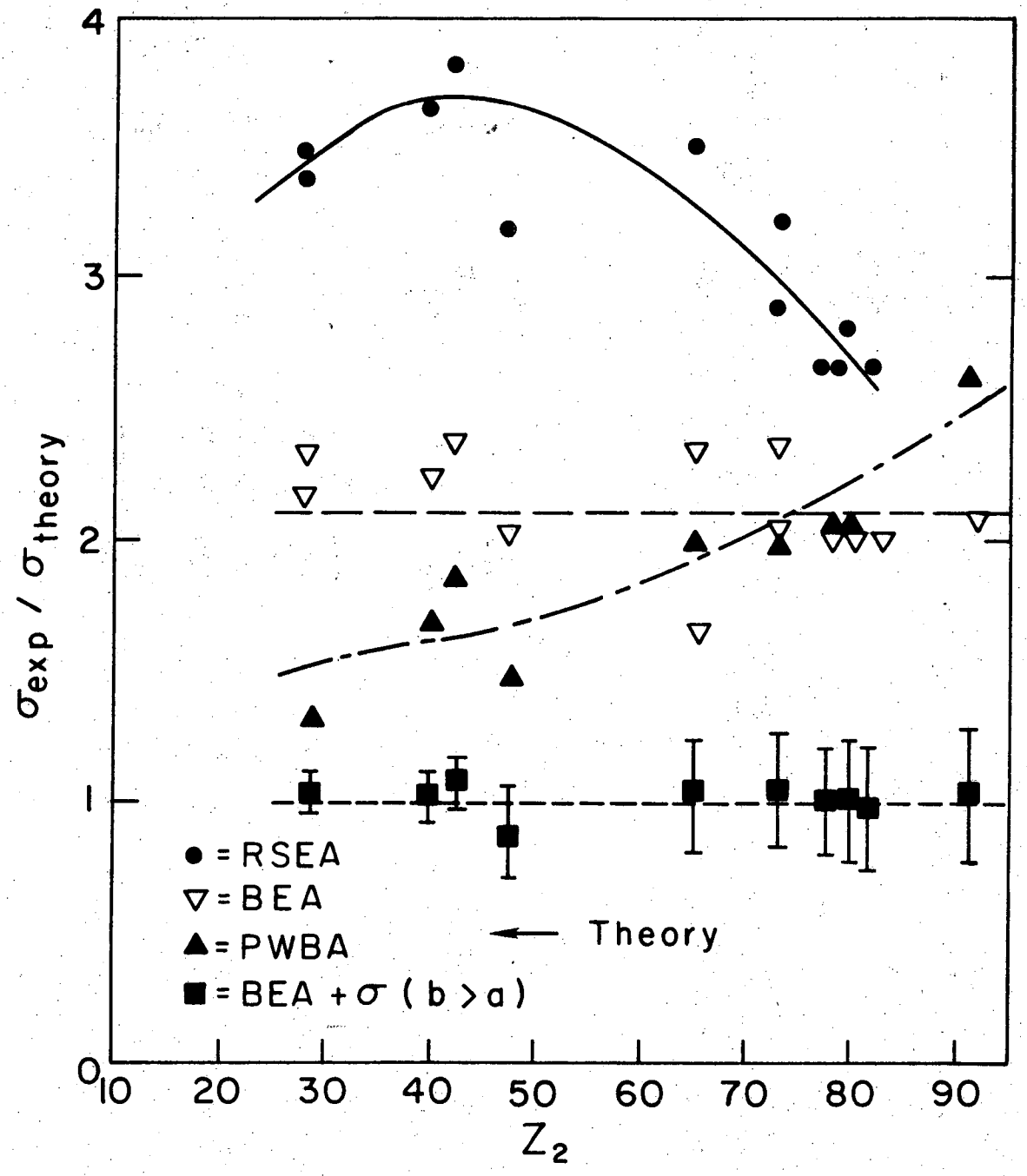

XBL 759-3988

Fig. 4

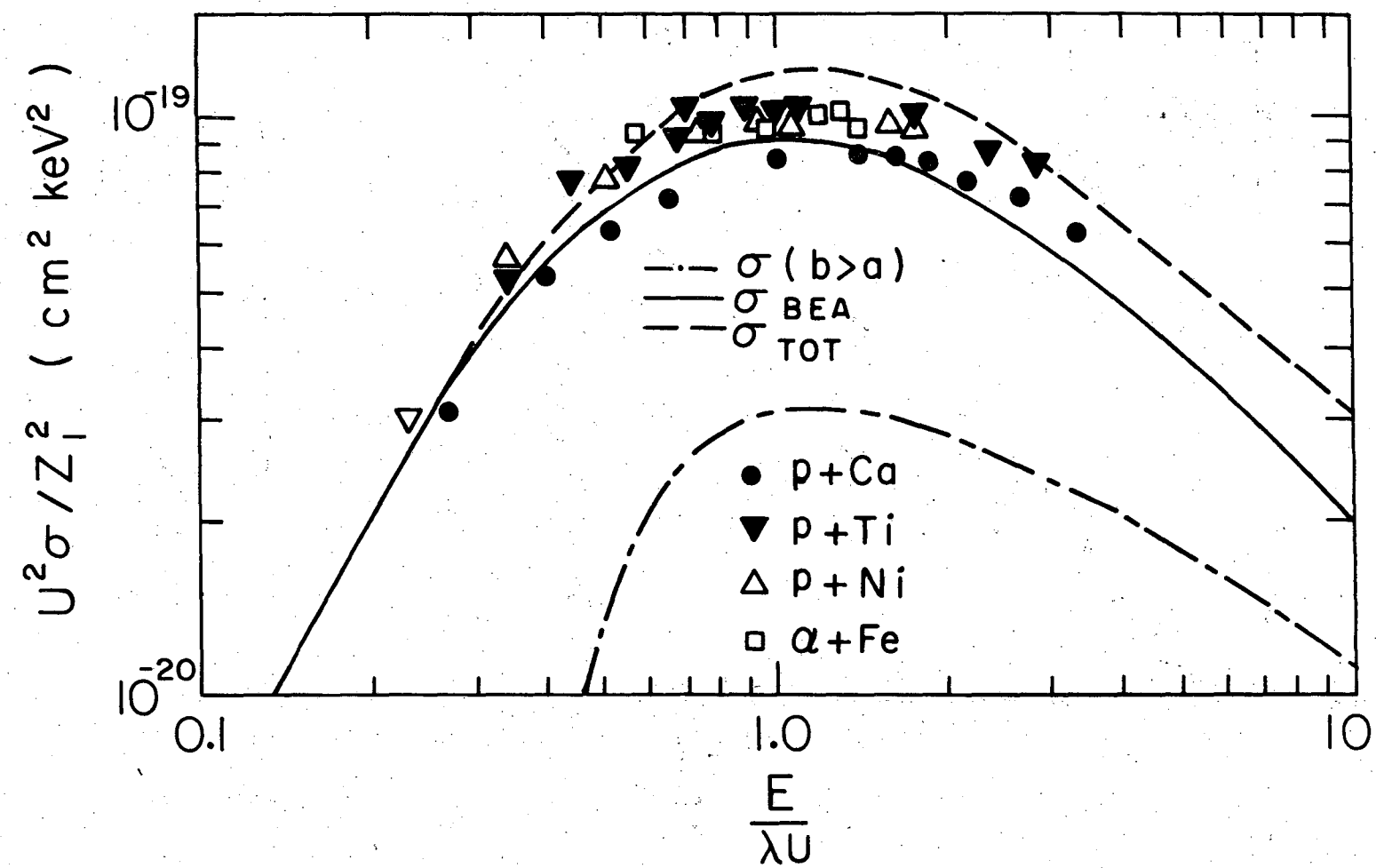

XBL759-3986

Fig. 5

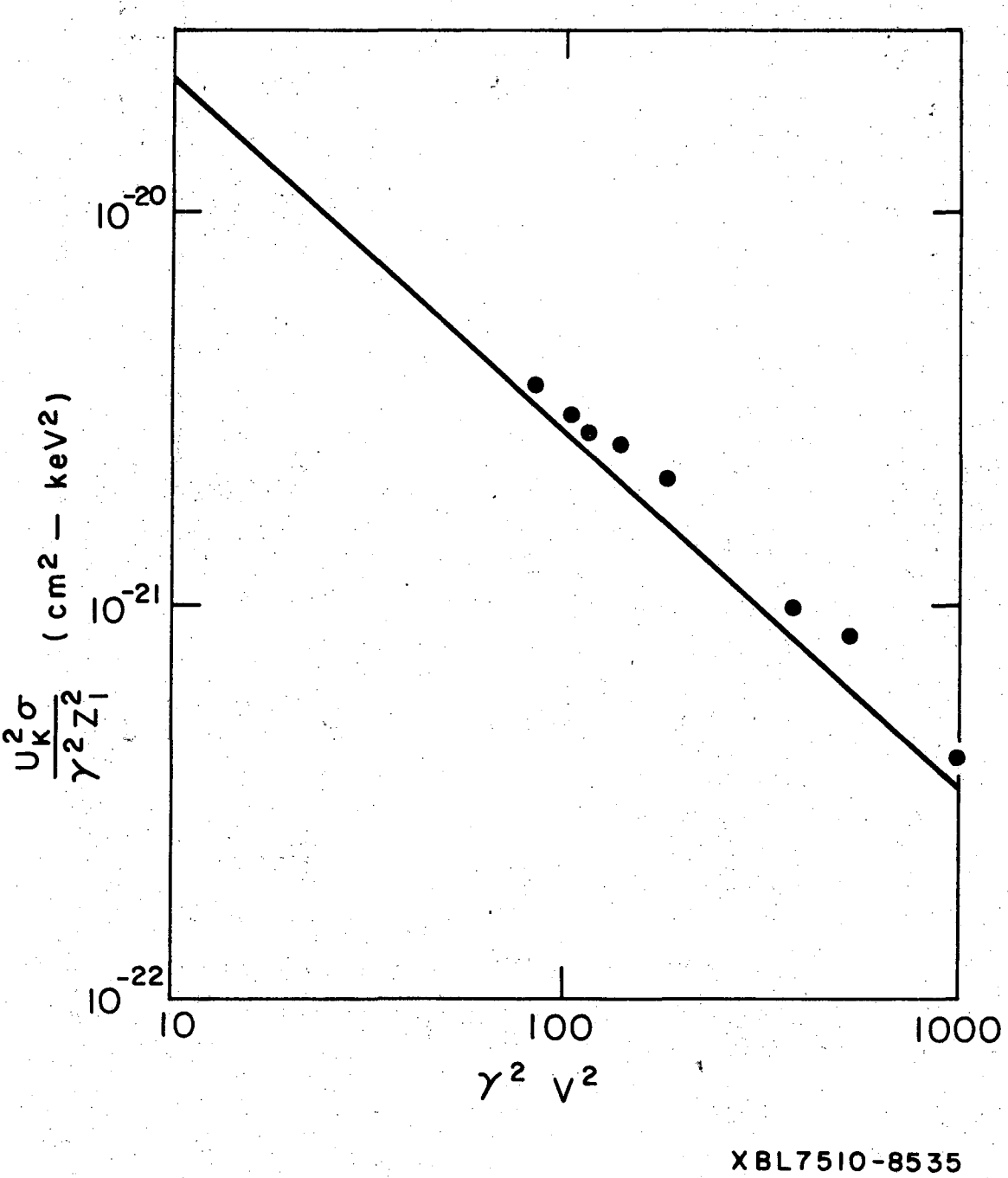

XBL7510-8535

Fig. 6

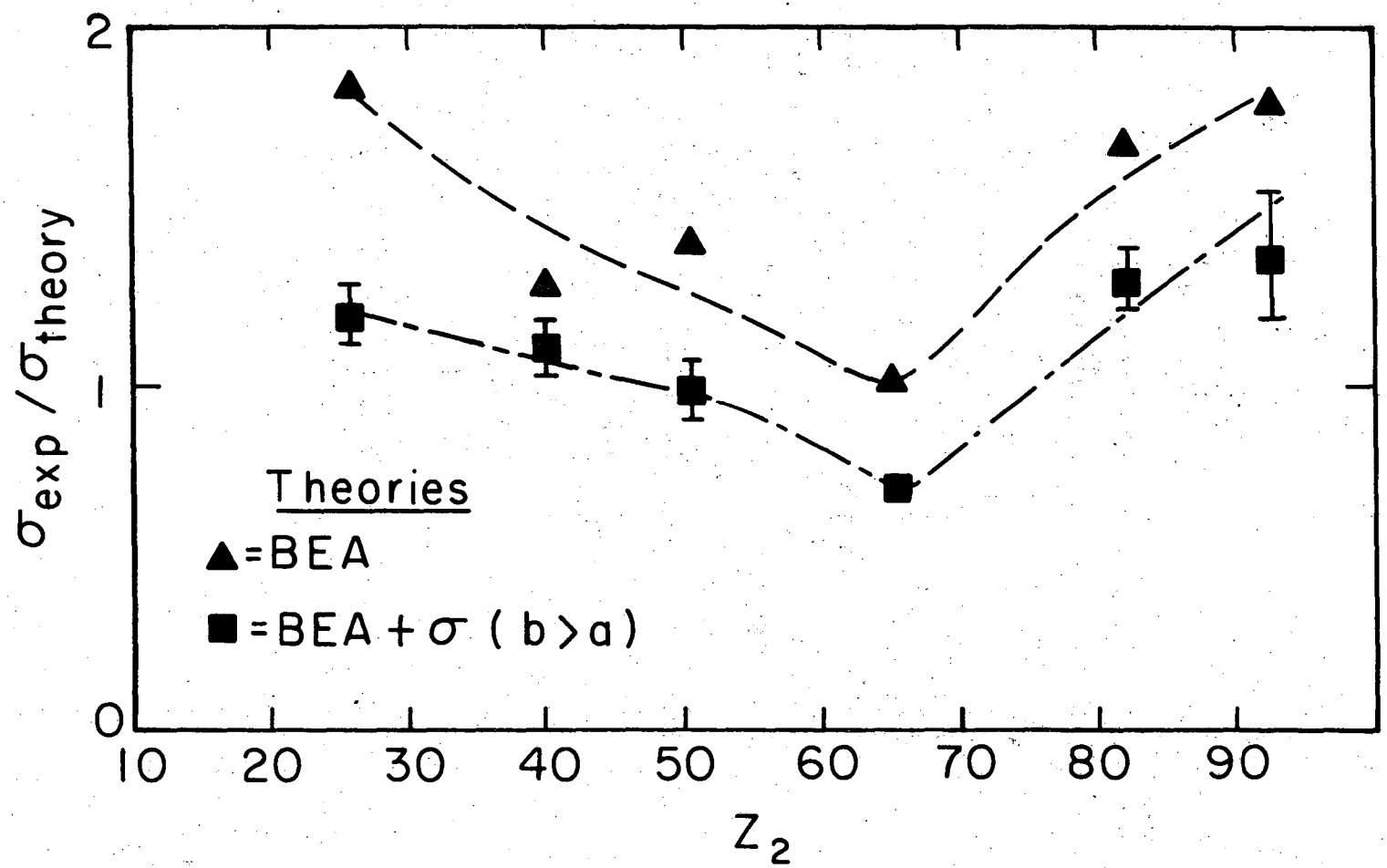

XBL759-3989

Fig. 7

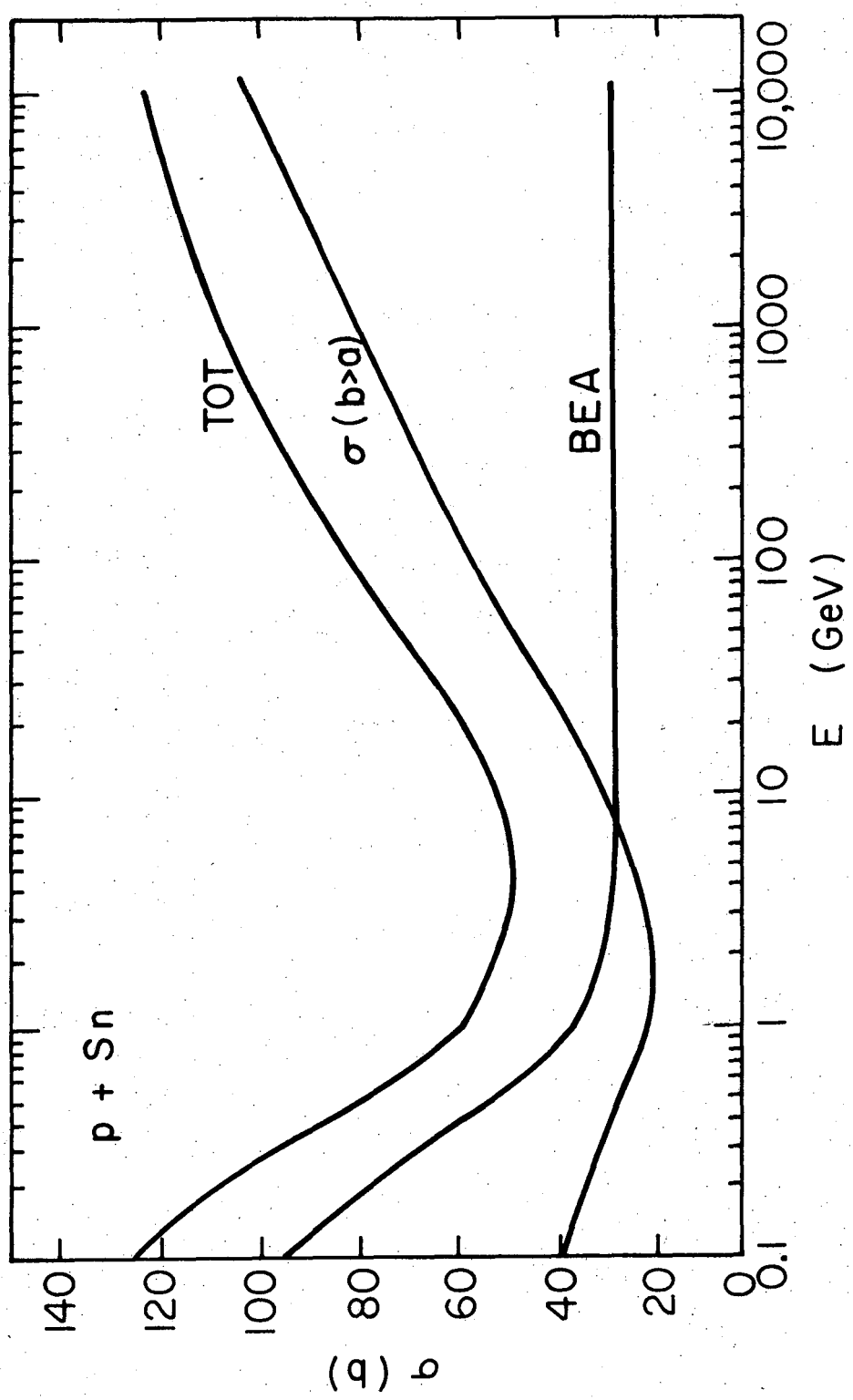

XBL759-3991

Fig. 8

0 0 0 0 4 4 0 0 2 3 3

LEGAL NOTICE

This report was prepared as an account of work sponsored by the United States Government. Neither the United States nor the United States Energy Research and Development Administration, nor any of their employees, nor any of their contractors, subcontractors, or their employees, makes any warranty, express or implied, or assumes any legal liability or responsibility for the accuracy, completeness or usefulness of any information, apparatus, product or process disclosed, or represents that its use would not infringe privately owned rights.

TECHNICAL INFORMATION DIVISION
LAWRENCE BERKELEY LABORATORY
UNIVERSITY OF CALIFORNIA
BERKELEY, CALIFORNIA 94720